



Determining push-off forces in speed skating imitation drills

Dominik Krumm¹ · Nicolas Kuske² · Maja Neubert¹ · Jens Buder¹ · Fred Hamker² · Stephan Odenwald¹

Accepted: 6 October 2021 / Published online: 28 October 2021
© The Author(s) 2021

Abstract

Speed skating takes place on ice rinks and is, therefore, dependent on seasonal conditions. To be able to train all year round, training in the summer months, when no ice rinks are available, consists mainly of athletics and endurance training as well as imitation drills. Imitation drills are exercises, e.g. on a slide board, which imitate the actual skating movement. To objectively evaluate the quality of the execution of these exercises, key performance indicators such as push-off forces need to be quantified. The aim of this work was to determine the push-off forces during speed skating imitation drills using pressure insoles in combination with machine-learning methods. A slide board is usually not instrumented. Here, the slide board was equipped with force plates to record the target variables, i.e. the push-off forces. The input variables to determine the push-off forces were recorded using plantar pressure insoles and triaxial accelerometers. Seven participants took part in the study. Two different machine-learning algorithms were compared. A non-linear deep neural network model and a linear multiple variable regression model. The models were trained using the obtained force–time curves. The linear regression model proved sufficient to predict the push-off forces. The relative difference between the measured and modelled maximum push-off force remained below 5%. This approach, based on a mobile and low-cost measurement system, allows a quantitative analysis of the athlete's technique/performance. Therefore, we expect the instrument to be a helpful tool for the training of speed skaters.

Keywords Machine learning · Winter sport · Speed skating · Ground reaction forces · Training control

1 Introduction

In speed skating, top performance consists of an optimum between power generation and minimal power loss due to air and ice friction [1]. To reduce the aerodynamic drag, athletes use a crouched skating position with low knee and trunk angles [2]. Since the friction between the skate blade and the ice is very low [3], athletes have to use the gliding technique to generate propulsion [4, 5]. This means that push-off forces against the ice must be generated in the direction perpendicular to the gliding direction of the skate [6].

The total power of the athlete is calculated from the work per stroke and the stroke frequency [6]. The work per stroke is determined by the lateral component of the push-off force, which is directed at right angles to the gliding direction [6]. The stroke frequency or cadence is determined as the number of push-offs per minute (ppm) [7]. The skating motion consists of a skating stroke, which is divided into the glide phase, the push-off phase, and a recovery phase [4]. The glide phase is characterised by the body being supported by one leg, which remains at an almost constant length. The push-off phase begins with the initiation of leg extension and ends with full leg extension when the skate blade lifts off the ice. In the recovery phase, the skate is returned to the starting position under the body [4].

The performance of speed skaters is maintained and maximised by regular training. Due to the varying physiological and neuromuscular demands, such training should include sport-specific training stresses [8]. However, winter sports athletes can struggle with access to the necessary training facilities during summer [8]. Therefore, speed skaters established alternative training methods that imitate one or more specific parts of the speed skating movement to maintain or

This article is a part of Topical Collection in Sports Engineering on Winter Sports, edited by Dr. Aimee Mears, Dr. David Pearsall, Dr. Irving Scher and Dr. Carolyn Steele.

✉ Dominik Krumm
dominik.krumm@mb.tu-chemnitz.de

¹ Sports Equipment and Technology, Chemnitz University of Technology, 09107 Chemnitz, Germany

² Professorship of Artificial Intelligence, Chemnitz University of Technology, 09107 Chemnitz, Germany

build their performance [9]. The so-called imitation drills train both technical and physiological skills.

It is possible to train the specific movement characteristics of speed skating outside the ice season using a slide board. The slide board is a non-instrumented horizontal board with a smooth surface and upright bars at both lateral ends, on which the skating motion (Fig. 1) can be imitated while athletes wear athletic shoes [9]. Athletes push-off from the bar located on one side of the board with one leg and then slide sideways to the other side. Once there, they push-off from the bar with their opposite leg. Although the friction of the slide board (0.13 ± 0.05 [7]) is four times as high as skating on ice (between 0.003 and 0.031 [3]), these imitation drills show a high degree of similarity to speed skating [9].

Quantitative recording of athlete performance parameters during training is commonly used to plan, monitor and control training interventions. In speed skating, quantitative information such as work per stroke as well as stroke frequency can provide relevant information about fatigue and performance. In 1982, van Ingen Schenau et al. [10] showed that the lateral push-off force determines the amount of useful work per stroke and that interindividual differences in performance are related to differences in push-off mechanics [6]. Push-off forces can thus be considered a valuable control parameter for effective training.

The established approach of recording ground reaction forces with a force plate in the laboratory does not fully reflect actual conditions during athletic activity [11]. Therefore, recording ground reaction forces under field conditions has recently become a frequent research topic [12]. The push-off forces in speed skating have been measured using instrumented skates [3, 13]. These skates had measuring elements made of aluminium with three temperature-compensated strain gauges between the shoe and the skate blade to register forces in both fore/aft and normal direction. The complete measurement system also consisted of a battery pack and a microcomputer, both worn on the skater's

back. While these are promising approaches, they rely on costly hardware and a complicated setup. The usability of these instrumented skates is also compromised outside of the winter season.

Alternative approaches to measuring ground reaction forces based on machine learning have already been used in the field of running. For example, Billing et al. [14] used artificial neural networks to determine ground reaction forces of four middle-distance runners. The input variables were the values measured by pressure sensors and the target variables were the ground reaction forces measured by a force plate. Jacobs and Ferris [15], as well as Savelberg and Lange [16], demonstrated that ground reaction forces can be determined with less than 10% deviation compared to a force plate using pressure insoles and artificial neural networks.

In this paper, a similar approach is applied to speed skating using the example of imitation drills on a slide board. The slide board, which was instrumented using two force plates, was chosen for two reasons. First, as mentioned earlier, the use of a slide board mimics the actual speed skating motion on ice [9]. Second, the movements can be performed at a stationary location under controlled conditions throughout the year. This makes it possible to record the target variables with consistent quality.

The aim of this work was to find out to what extent it is possible to determine the push-off forces of an athlete during training on a regular slide board that does not provide force plate sensor data. Based on pressure insoles and their combination with machine-learning methods, a mobile, low-cost, and easy-to-use measurement system for determining the push-off forces was developed.

2 Methods

A slide board was instrumented to record the target variables, i.e. push-off forces and times. The slide board (2.5 m wide, 1.25 m deep, and 0.25 m thick) with a polyethylene

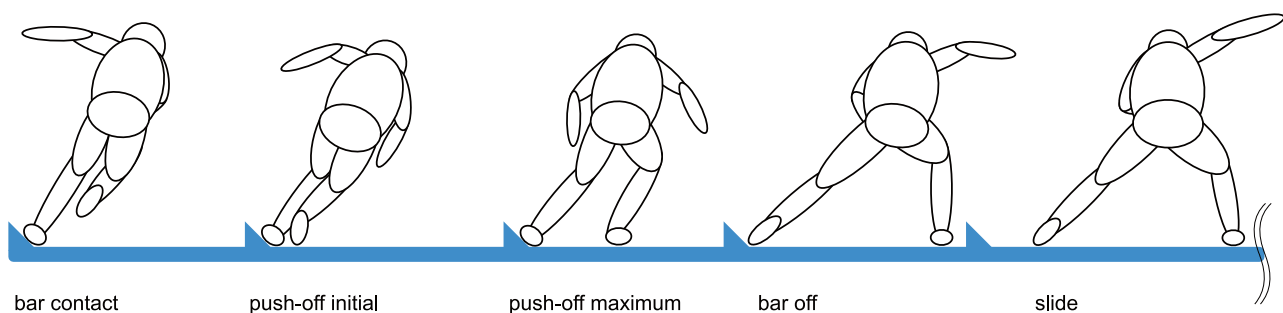


Fig. 1 The characteristic phases of the speed skating imitation drill on a slide board, shown for the left side. The sliding movement from the opposite side of the slide board ends with the bar contact of the

left leg. The push-off phase begins with push-off initial. The push-off force increases until push-off maximum is reached. The slide phase begins with the release of the left leg from the bar

surface was mounted at both ends on two force plates with built-in amplifiers (Fig. 2). The control of the first force plate (model 9287BA, Kistler Instrumente AG, Winterthur, CHE), which was connected to a data acquisition system (Lock+, Oxford Metrics, Oxford, GBR), was performed using Nexus 2 software (Oxford Metrics, Oxford, GBR). The control of the second force plate (model 9286BA, Kistler Instrumente AG, Winterthur, CHE), which was connected to another data acquisition system (imc CRONOS PL-2, imc Test & Measurement GmbH, Berlin, DEU), was performed using imc DEVICES software (imc Test & Measurement GmbH, Berlin, DEU). The resulting medio-lateral force (F_x), calculated as the sum of the two separately measured medio-lateral forces of each plate (F_{x1} , F_{x2}), was used as the target variable for the push-off force.

The input variables for determining the push-off force were obtained from 16 plantar pressure signals (P_n , where n represents the sensor channel from 1 to 16) and two tri-axial accelerometers (a_{xL} , a_{yL} , a_{zL} , a_{xR} , a_{yR} , a_{zR}). Plantar pressures were measured by two pressure insoles (each 0.8 mm thick and weighing 7 g) inserted into the athletes' sports shoes. Each pressure insole consisted of eight individual pressure sensors (Smart footwear sensors/HD 002, IEE, Echternach, LUX). Sensor readings in each sole were recorded and synchronised by mobile measurement systems (each 50 mm long, 30 mm wide, 19 mm high and weighing 30 g) with integrated accelerometers that were attached

to the athletes' ankles. The mobile measurement systems were developed within our research group [17]. The sensors were controlled using the ENVISIBLE software (Envisible Steinbeis-Forschungszentrum Human Centered Engineering, Chemnitz, DEU).

Seven participants (one female and six males, with mean age and standard deviation of 34 ± 11 years, and a mass of 76.1 ± 8.8 kg) with different experience levels participated in this study (Table 1). The experience level refers to a participant's ability to perform the correct technique for speed skating imitation drills on a slide board, rather than fulfilling physiological requirements (Table S1 in Online Resource). The study was conducted in accordance with the ethical standards of the Behavioural and Social Sciences Ethics Board of the Chemnitz University of Technology. All participants took part voluntarily and provided informed consent.

The speed skating imitation drills were performed ten times by each participant on each of two separate measurement days. One trial consisted of five complete push-off phases per leg on the instrumented slide board while wearing the pressure insoles. Each trial lasted about 17 s. Before the trials, participants warmed up and became accustomed to the slide board. Since conditioning was recommended for the sensors used in the pressure insoles [18], the so-called Foot Sensing Resistors (FSR) sensors, this took place immediately before the actual imitation drills. Conditioning, i.e. prior loading of the sensors, is

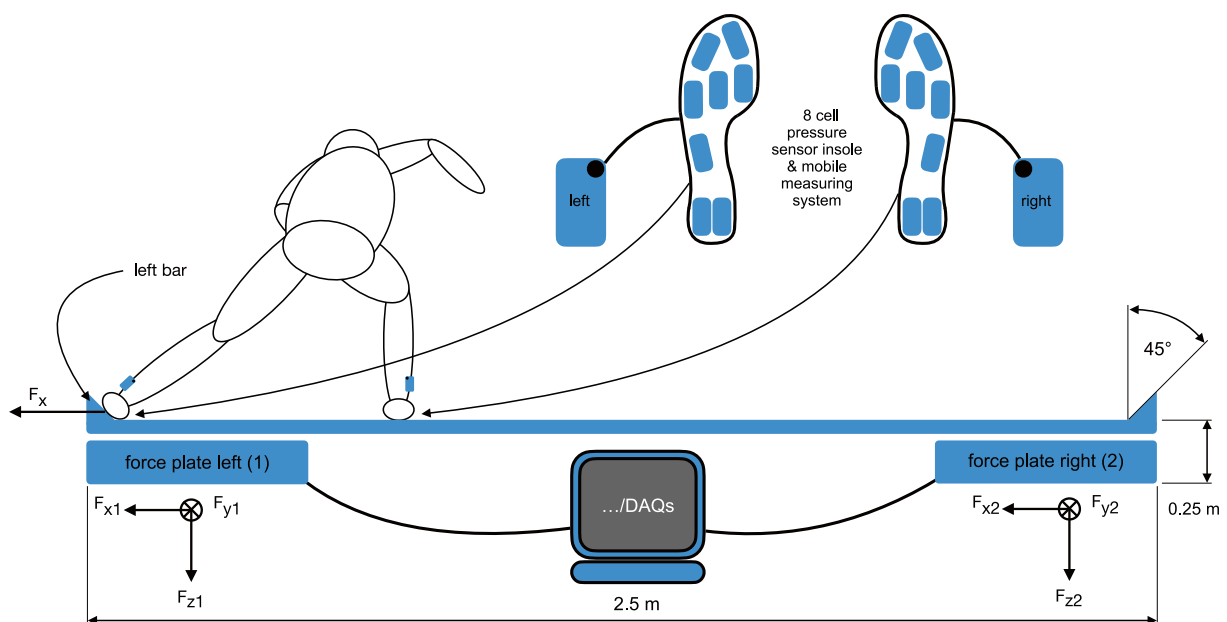


Fig. 2 Schematic representation of the test setup. The slide board was instrumented with two force plates to measure the target variables, i.e. resulting medio-lateral force and times during the speed skating imitation drill. Both force plates were connected to data acquisition systems. The input variables, i.e. plantar pressure signals, were

recorded by two thin pressure insoles, each with eight pressure sensors, inserted into the athlete's shoes. The insoles were each operated by a small mobile measurement system with integrated tri-axial accelerometers that was attached to the side of the athlete's legs

Table 1 Detailed information on participating athletes including anthropometric data and their experience level classification

Participant id	Gender	Age (years)	Body weight (kg)	Body height (m)	Shoe size (UK)	Insole size	Experience level
1	Male	48	80.2±0.4	1.80	10	XL	2
2	Female	31	74.1±0.7	1.74	7.5	L	1
3	Male	43	77.4±0.1	1.87	10.5	XL	2
4	Male	36	94.6±1.3	1.86	10.5	XL	4
5	Male	43	71.4±0.6	1.76	8	L	2
6	Male	18	68.6±1.2	1.74	9.5	XL	3
7	Male	19	66.4±0.0	1.79	9	L	3

The body weight data refers to the mean plus/minus the standard deviation

intended to ensure that the sensors provide repeatable results during testing. For this purpose, athletes first stepped onto the slide board with one leg from a double-legged stance and held this position for 2 s without movement before the second leg followed. During the trials, athletes wore socks over their sport shoes to reduce the coefficient of friction on the slide board. Both target and input variables were recorded at 100 Hz. Although athletes were asked to adopt the crouched skating position, body posture was not controlled in this study. All tests were performed within 6 months.

The measurement data were then pre-processed to manually synchronise the three different measurement systems. For synchronisation, the curves of the vertical forces (F_{z1} , F_{z2}) of each force plate and the pressure sum of each insole during the conditioning phase were considered. The characteristic deflection in each curve at the beginning of the single-leg stance on the slide board was automatically determined using MATLAB R2020b (The MathWorks Inc., Natick, MA, USA) and used as a starting point for all measurement systems. In individual cases, the course of the medio-lateral forces was also included in the determination of the exact time point. After synchronisation, the medio-lateral force data from the two individual force plates were combined to form the total medio-lateral force (F_x).

The following key performance indicators (KPI) were derived from the push-off force–time curve of the trimmed data sets to characterise the imitation drill technique (Fig. 3): force at bar contact (F_{BC}), time at bar contact (t_{BC}), force at push-off initial (F_{POi}), time at push-off initial (t_{POi}), force at push-off maximum (F_{POmax}), time at push-off maximum (t_{POmax}), force at bar off (F_{BO}) and time at bar off (t_{BO}). Time at bar contact was also used to calculate the stroke frequency (f). The bar contact was identified as a local maximum and the bar off event as a local minimum in the push-off force. The initial push-off event was identified as a local minimum in the measured push-off force between bar contact and push-off maximum.

It is possible to extract the approximate times of each KPI during a trial on the slide board using only the pressure and acceleration sensor (see “Results” section). However, it is unclear how to transform the sensor data into the correct force amplitude at these particular time points. Modern machine-learning methods rely on thousands of data points to find the optimal model parameters. To solve this problem, the learning algorithms used here were trained to optimally predict the complete force–time curve by minimising the root mean squared error (RMSE) between the measured and the modelled force at each time point. First, the training of the algorithm was completed and the parameters of the model were optimised. Second, the time points that denote each KPI were manually derived from the sensor curves (not from the force plates). Finally, the sensor values at these time points were used as input to the model to predict the specific KPI force values.

Each participant was modelled separately. All models were trained using the concatenated data of the 16 insole pressure sensors collected during the first six trials on the slide board on the first of the participant’s two measurement days. The ankle acceleration sensors did not substantially improve the models and were excluded from training. To use only data from the regular movement execution on the slide board, the data before the second sliding stroke and the data after the penultimate sliding stroke were truncated for each trial. Each model was trained to minimise the RMSE between one output variable and the measured medio-lateral force–time curve.

To avoid overfitting, machine-learning researchers typically test their models on different data than that used for training. Approaches which predicted athlete’s ground reaction forces trained and tested their models on data recorded on 1 day [14–16]. This procedure can be insufficient if the athlete wants to use the model again on another day. Several factors might affect the model’s accuracy in between these days. To counteract this potential shortcoming, the accuracy of our models was tested on the four remaining trials of the

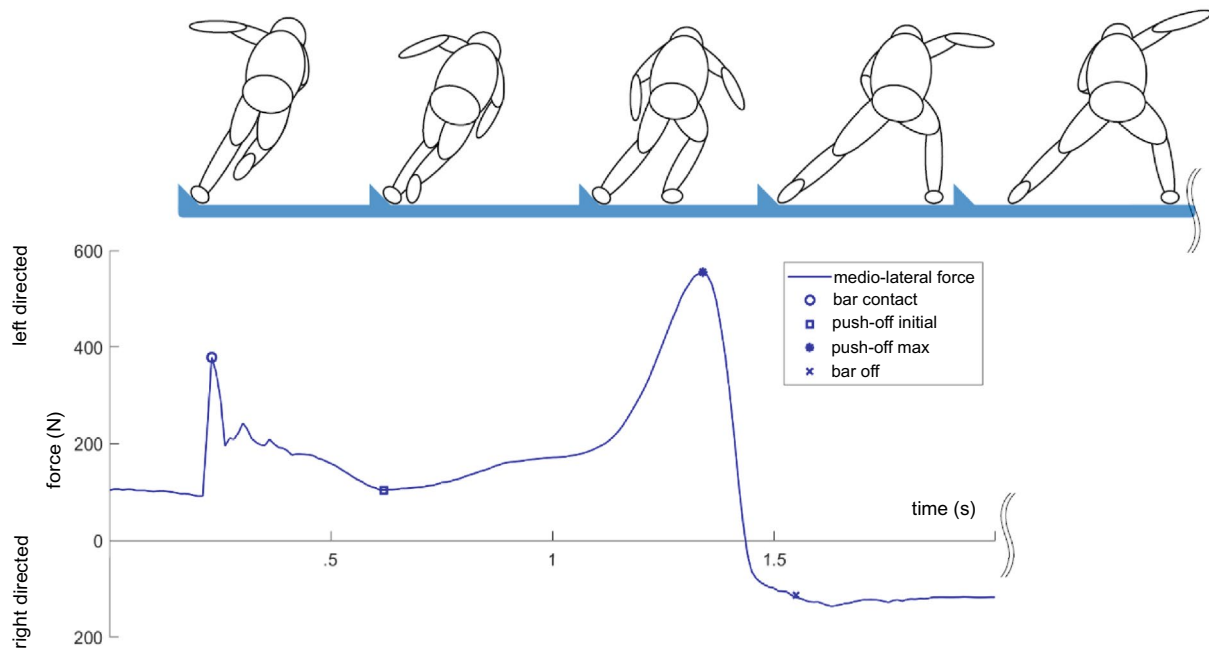


Fig. 3 Medio-lateral force–time curve of the speed skating imitation drill on the slide board with key performance indicators drawn in and schematic representation of the phases. Note that the symbol ‘o’ indi-

cates the bar contact (BC), ‘□’ indicates push-off initial (POi), ‘**’ indicates push-off maximum (POmax), and ‘x’ indicates bar off (BO)

first measurement day and on all ten trials of the second measurement day. The interval between the first and second measurement day lasted from 3 weeks to 6 months.

Two different machine-learning algorithms were compared. A non-linear deep neural network model and a linear multiple variable regression model. Deep neural networks are the backbone of virtually all modern machine-learning algorithms [19–21]. However, classical multiple linear regression is also still used as a modelling tool in academia and industry [22–25]. The advantage of linear regression models is their simplicity. The user can understand what the model is doing and the machine can quickly compute the optimal parameter values. Furthermore, if the functional relationship between the independent and dependent variables is almost linear, a deep neural network will not outperform a linear model.

The basic building blocks for the deep neural network model used were provided by and implemented in the Keras 2.4 machine-learning library [26]. The models were run using Python 3.9 on a quad-core 1.80 GHz Intel i7-10510U processor with 32 GB RAM. Deep networks with varying numbers of hidden layers (1–5) and several different activation functions were compared. All networks were trained using Nesterov’s stochastic gradient descent [27, 28] with decay and momentum. Of the model architectures tested, a network with 1 hidden layer of 20 artificial neurons or units, each using a rectified linear activation function, proved to be optimal.

A comparison of the performance (using the RMSE) of the optimal deep neural network and a linear model implemented in Python using the sci-kit 0.24.2 machine-learning library [29] was done. The linear model performed equally well or slightly better than the deep neural network. The characteristic curve describing the ratio of voltage to pressure of the insole sensors was logarithmic, but could be well approximated as linear up to 1 V. Since only 2% of the measured sensor data had voltage values above this 1 V threshold, the linear approach seems to be sufficient to model the relationship between pressure sensors and force.

Consequently, all data analysed in the results were produced using linear multiple regression. For simplicity, the models used throughout the analysis were implemented in MATLAB R2020b using its linear machine-learning model libraries. An explorative comparison of a linear mixed-model approach in MATLAB with trial as a grouping factor also showed no improvement in performance. The “simple” multiple linear regression model performed best.

In the search for further optimisation of the performance of the linear regression model, it was found that certain KPIs were better predicted when the model was trained only on characteristic intervals of the force–time curve. Only for bar off (BO) the optimal model parameters were found when the machine-learning algorithm was trained on the complete data as described above. This model, trained on the complete data, will be referred to as the skate model. The remaining performance indicators in terms of bar contact

(BC), push-off initial (POi) and push-off maximum (POmax) events, were best predicted when the model was trained only on the data between bar contact and the maximum push-off amplitude. This model, trained only on data between the bar contact and the maximum push-off amplitude, will be referred to as the push-off model. The push-off model was further improved by modelling the left leg push-off data separately from the right leg data. For each participant, a total of three models were trained on their data. One skate model using the complete data and two push-off models, each trained on the intervals from t_{BC} to t_{POmax} for each leg. Altogether, 21 multiple linear regression models were trained and tested. All model parameters and complete force–time curve RSMEs are given in the Online Resource.

Statistical analyses were performed to identify meaningful differences between the measured and modelled KPI of the test data. Specifically, mean values, standard deviations, RMSE, absolute differences (δ) and relative differences (Δ) were calculated to make informed statements about the predictability of push-off forces combining pressure insoles and machine-learning methods. The KPIs were additionally examined with respect to various factors that may influence the predictability. These independent factors included the participants, the day of measurement, the number of trials, and the side of the leg.

All data and analysis scripts were uploaded to a public repository on OSF (Open Science Framework from the

Center of Open Science) and can be accessed at <https://osf.io/kaghn/>.

3 Results

The push-off force–time curves and characteristic KPIs of the speed skating imitation drills on a slide board could be modelled for the seven participating athletes (Fig. 4). Only test trials (four trials per participant on measurement day one and all ten trials per participant on measurement day two) were used for the comparison of measured and modelled KPIs. The total maximum push-off force (F_{POmax}) was 575 N with a standard deviation of 85 N. The modelled value was 542 ± 103 N (Table 2). This total force was calculated as the mean of all factors such as participant, day of measurement, number of trial and leg side. The total relative difference between the amplitude of measured and modelled F_{POmax} was under 5% (Table 3).

If one considers the difference in amplitude between the measured and modelled push-off force as a function of individual factors, larger differences can be seen in some cases. For the factor participant, the differences vary between $0.0 \pm 10.9\%$ (p #4 with the highest experience level) and $12.9 \pm 11.0\%$ (p #1). For the factor day of measurement, the differences between measurement and model were smaller on the second measurement day than on the first

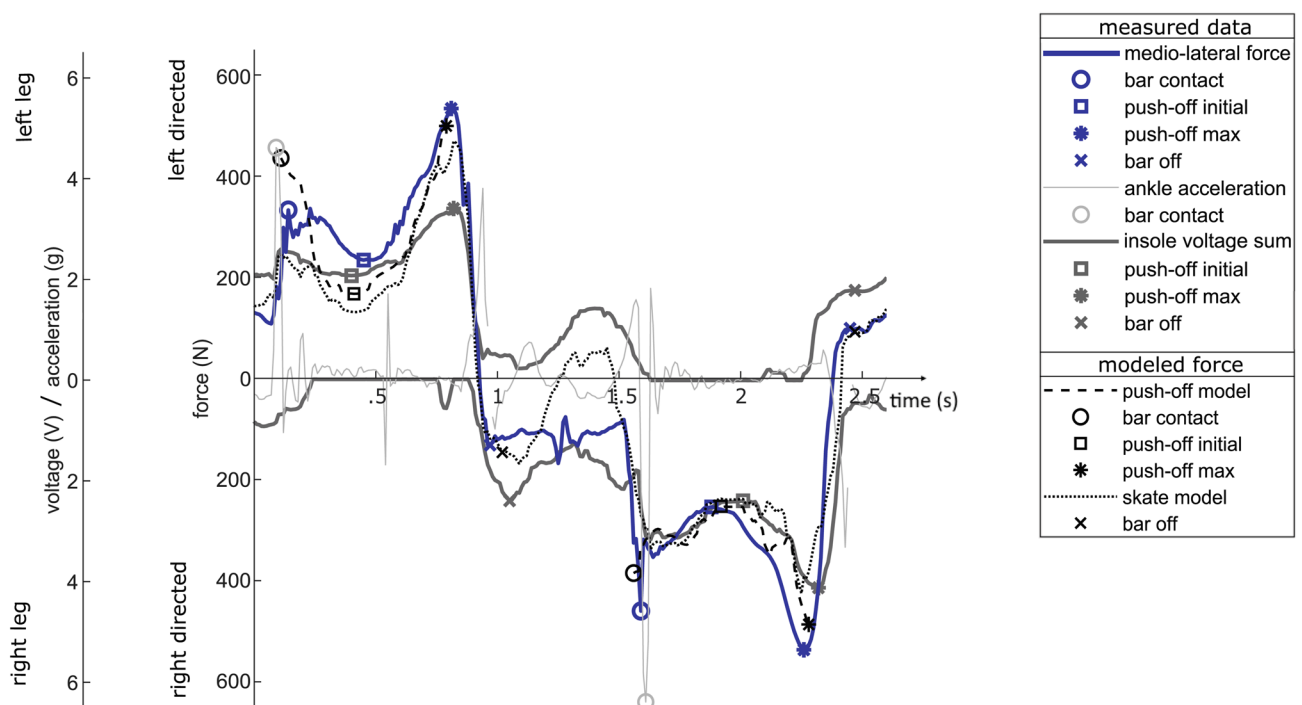


Fig. 4 Measured and modelled parameters of trial number three on the second measurement day of participant one. Only one skate slide is shown for each side. For simpler display the ankle acceleration is only shown for the leg on the bar contact side

Table 2 Maximum push-off forces (F_{POmax}) and stroke frequencies (f)

		F_{POmax} (N)			f (ppm)		
		Measured	Modelled	Δ (%)	Measured	Modelled	Δ (%)
(a)	Total	575 ± 85	542 ± 103	4.9 ± 17.7	22.8 ± 4.0	22.8 ± 4.0	-0.1 ± 2.7
(b)	Left leg	572 ± 84	564 ± 119	0.7 ± 18.6	22.9 ± 3.9	22.9 ± 3.9	-0.1 ± 2.0
	Right leg	579 ± 85	520 ± 79	8.9 ± 15.9	22.7 ± 4.0	22.7 ± 4.1	-0.1 ± 3.2
(c)	Day 1	572 ± 83	527 ± 89	7.3 ± 14.5	22.3 ± 3.9	22.4 ± 4.0	-0.2 ± 3.7
	Day 2	577 ± 87	548 ± 108	3.8 ± 18.8	23.0 ± 4.0	23.0 ± 4.0	-0.1 ± 2.1
(d)	p #1	537 ± 39	465 ± 45	12.9 ± 11.0	21.2 ± 1.6	21.2 ± 1.7	-0.3 ± 2.8
	p #2	676 ± 72	615 ± 89	8.2 ± 15.5	23.7 ± 1.2	23.7 ± 1.3	0.0 ± 2.1
	p #3	523 ± 36	465 ± 129	11.2 ± 22.8	15.5 ± 1.1	15.5 ± 1.1	0.0 ± 1.6
	p #4	590 ± 51	587 ± 60	0.0 ± 10.9	23.3 ± 1.3	23.3 ± 1.4	-0.3 ± 2.2
	p #5	628 ± 43	551 ± 75	11.9 ± 13.6	25.0 ± 1.4	25.0 ± 2.0	-0.2 ± 5.0
	p #6	621 ± 33	614 ± 110	0.9 ± 19.1	29.1 ± 1.3	29.1 ± 1.3	-0.1 ± 1.5
	p #7	462 ± 36	507 ± 47	-10.5 ± 14.2	22.5 ± 1.2	22.5 ± 1.3	0.0 ± 1.8

Given are the means and standard deviations of the measured target variables derived from the force plates, the modelled variables predicted from the pressure input variables of the test data, and their relative differences (Δ); (a) F_{POmax} independent of participant (p), day, trial and leg; (b) F_{POmax} independent of participant, day and trial; (c) F_{POmax} independent of participant, trial and leg; (d) F_{POmax} independent of day, trial and leg

Table 3 Mean and standard deviation for absolute difference (δ) between measured target variables derived from the force plates and the modelled variables for bar contact times (t_{BC}), push-off initial times (t_{POi}), push-off maximum times (t_{POmax}) and bar off times (t_{BO});

(a) differences independent of participant (p), day, trial and leg; (b) differences independent of participant, day and trial; (c) differences independent of participant, trial and leg; (d) differences independent of day, trial and leg

		t_{BC} (s)	t_{POi} (s)	t_{POmax} (s)	t_{BO} (s)
(a)	Total	0.01 ± 0.06	-0.03 ± 0.12	0.01 ± 0.05	-0.01 ± 0.06
(b)	Left leg	0.00 ± 0.05	-0.02 ± 0.11	0.01 ± 0.05	-0.01 ± 0.06
	Right leg	0.02 ± 0.06	-0.05 ± 0.13	0.01 ± 0.05	0.00 ± 0.06
(c)	Day 1	0.01 ± 0.06	-0.01 ± 0.10	0.01 ± 0.05	0.00 ± 0.05
	Day 2	0.01 ± 0.05	-0.04 ± 0.13	0.01 ± 0.05	-0.01 ± 0.06
(d)	p #1	0.02 ± 0.07	-0.01 ± 0.10	0.02 ± 0.06	-0.02 ± 0.05
	p #2	0.02 ± 0.04	0.01 ± 0.06	0.02 ± 0.04	0.01 ± 0.05
	p #3	0.00 ± 0.05	-0.05 ± 0.20	0.00 ± 0.05	0.02 ± 0.06
	p #4	-0.02 ± 0.06	-0.06 ± 0.15	0.01 ± 0.05	-0.02 ± 0.06
	p #5	0.00 ± 0.08	-0.04 ± 0.09	0.01 ± 0.05	-0.05 ± 0.06
	p #6	0.00 ± 0.03	-0.07 ± 0.12	0.01 ± 0.03	0.01 ± 0.04
	p #7	0.01 ± 0.04	-0.02 ± 0.10	0.01 ± 0.07	0.00 ± 0.04

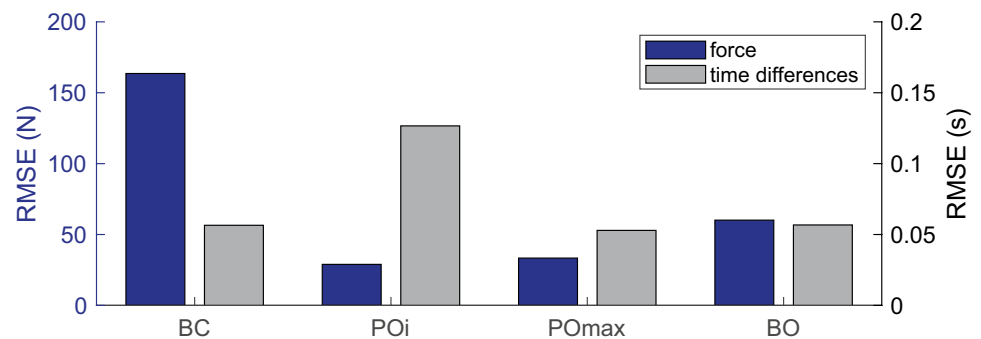
measurement day. Differences were also apparent when the leg side factor was considered in isolation. In particular, the mean relative difference for the left leg (0.7%) was smaller than for the right leg (8.9%). Another result that can be derived from the table is that the standard deviation ranged consistently between 10.9% and 22.8%, regardless of the other factors. The total amplitudes and relative differences of the other KPIs are listed in the Online Resource (Table S2 to S4).

The KPIs that denote the timing of events were predicted accurately. The total mean absolute error between the predicted KPIs derived from the modelled variables and the KPIs determined from the measured variables was less than

0.03 s (Table 3). Looking at the individual factors in isolation, one finds that with the exception of the push-off initial times (t_{POi}) for participant four (-0.06 s) and six (-0.07 s), all mean absolute differences were less than or equal to 0.05 s. This was also reflected in the small relative differences for the stroke frequencies (Table 2) calculated from the times at bar contact (t_{BC}).

The total RMSEs of force amplitudes and time differences of all KPIs were predicted with varying accuracy by the multiple linear regression models (Fig. 5). Push-off initial and push-off maximum show the smallest deviation in amplitude with 29 and 33 N, respectively. The deviation of the predicted and measured medio-lateral force during

Fig. 5 Total root mean square errors (RMSE) of the force amplitudes and time differences for measured target variables and the modelled variables for bar contact (BC), push-off initial (POi), push-off maximum (POmax) and bar off (BO)



contact with the bar at the edge of the slide board was about five times as large with 164 N. When the athlete leaves the bar again, the RMSE was 60 N. In the time parameters, t_{POi} shows the largest error with 0.13 s. All other KPI timing errors remain at about 0.05 s (RMSE of t_{BC} = 0.057 s; RMSE of t_{POmax} = 0.053 s; RMSE of t_{BO} = 0.057 s). In summary, not all KPIs can be determined equally well using only sensor data and machine-learning methods, but most errors remain small.

4 Discussion

The aim of this work was to determine the push-off forces that occur during speed skating imitation drills with the help of a mobile measurement system using machine learning. The intention behind this work was to assist athletes striving to improve their speed skating performance. Novel technological tools allow for quantitative analysis of the athlete's technique/performance. At the outset of this study, the push-off force as a key performance indicator could only be measured with force plates or instrumented skates. However, since most athletes have limited access to these instruments, the goal of this study was to provide a way to measure this key performance indicator using an alternative, low-cost, mobile and easy-to-use measurement system.

Characteristic KPIs for the skate movement on a slide board were determined and compared with the KPIs determined by a force plate. This comparison showed that the characteristic values matched the measured values well. However, it also revealed the limitations of the models used. For each athlete, three different models had to be trained to predict the individually measured medio-lateral force with a good agreement. In addition, different KPIs were predicted to varying degrees. On the one hand, the maximum push-off force (F_{POmax}), an apparently important parameter to characterise the performance of a skate stroke during the speed skating imitation drill, was well determined. On the other hand, the measured and modelled forces at contact with the slide board bar (F_{BC}) showed large deviations. The timings that are important for determining the different events,

including the derived stroke frequency, could again be predicted well.

The total relative difference between the measured and modelled maximum push-off force was under 5%. We consider this measurement error acceptable for practical applications. To our knowledge, push-off forces of imitation drills on the slide board have not previously been analysed, and thus no quantitative parameters are available to assess imitation drills. Other scientific papers dealing with the prediction of ground reaction forces could be used for comparison. Jacobs and Ferris [15], as well as Savelberg and Lange [16] showed that their models can predict ground reaction forces with under 10% deviation. Considering all KPIs investigated, the approach presented here shows similar accuracy. We believe that this system, which only requires the use of pressure insoles and the subsequent application of linear machine-learning models, is well suited to be used in training for continuous monitoring of athletes' performance.

Using the trials of the second measurement day, whose data were not used to create models, we showed that the models can be reliably applied to new trials after they have been trained for a specific athlete. The individual models generalise well over time. However, the models do not generalise well across all athletes. The push-off and skate models created for one athlete cannot be transferred to or used by other athletes without affecting the performance of the model. This circumstance was deliberately accepted, as otherwise a study with a much larger study population would have been required. Even with this larger study population, one could not have been sure that generalisable models would have been obtained. The search for optimal parameters for a global model could be the subject of future work. Here, the level of experience could prove to be an important meta-parameter.

Since a low-cost measurement system based on thin, flexible sensor cells was used for these measurements, the question arises as to how reliable the entire measurement system can be. The basis of the employed measurement system is FSR sensors. It is known that the sensor output changes during the first few times being loaded. However, by conditioning the sensor before the actual measurement, this artefact

can be counteracted [18]. Another problem with this type of sensors is drift, which is the change of a metrological property of a measuring instrument over time. There is no indication of the amount of drift in the sensor data sheet [30]. According to the manufacturer, the FSR sensors used are high-dynamic sensors that have been specifically designed for in-shoe pressure measurement applications. Since these sensors have a high degree of environmental and mechanical robustness with a relatively low hysteresis at 8%, we expect that the drift will not have an excessively negative impact on the reliability of the measurement system. In conclusion, it can be assumed that the measurement system is reliable for the intended applications.

Another limitation of this study was the small and unbalanced population sample. For example, only one participant with the lowest and one with the highest experience level participated. Only one female was among the total of seven participants. For this reason, no conclusions can be drawn from the results as to whether and to what extent experience or gender differences have an influence on the prediction of push-off forces. The effect of experience and gender could be investigated in follow-up studies.

5 Conclusion

This work has shown that it is possible to accurately predict the push-off forces of an athlete during speed skating imitation drills using pressure insoles and machine-learning models. Furthermore, some individual KPIs can be determined with a higher accuracy than others. Although there are already technical solutions for measuring push-off forces on ice, e.g. instrumented skates, we plan to transfer our presented solution from the slide board to speed skating in the future. Such a solution could have advantages over instrumented skates. Unlike instrumented skates, the system developed here could be used in combination with the athletes' individual skates. The mass of the complete measurement system would be lower, allowing a standard training experience. We believe it is unlikely that our combined system of pressure insoles and machine-learning models can reach the accuracy of calibrated instrumented skates or immobile force sensors. Nevertheless, if we are able to match or exceed the accuracy demonstrated here for imitation drills on the slide board also for speed skating on ice, our instrument could equally become a valuable tool for training speed skaters on ice.

Supplementary Information The online version contains supplementary material available at <https://doi.org/10.1007/s12283-021-00362-1>.

Funding Open Access funding enabled and organized by Projekt DEAL. This project was funded with research funds from the Bundesinstitut für Sportwissenschaft based on a resolution of the Deutscher

Bundestag (German Bundestag)—Project-ID ZMVI4-071503/20-21 and co-financed with tax funds on the basis of the budget passed by the Sächsischer Landtag. (Saxon state parliament)—Project-ID 100378180 and from the Deutsche Forschungsgemeinschaft (DFG, German Research Foundation)—Project-ID 416228727—SFB 1410.

Availability of data and material The data were uploaded to the repository on OSF (Open Science Framework from the Center of Open Science) and can be accessed at the following link: <https://osf.io/kaghn/>.

Code availability The analysis scripts were uploaded to the repository on OSF (Open Science Framework from the Center of Open Science) and can be accessed at the following link: <https://osf.io/kaghn/>.

Declarations

Conflict of interest The authors declare no conflict of interest.

Open Access This article is licensed under a Creative Commons Attribution 4.0 International License, which permits use, sharing, adaptation, distribution and reproduction in any medium or format, as long as you give appropriate credit to the original author(s) and the source, provide a link to the Creative Commons licence, and indicate if changes were made. The images or other third party material in this article are included in the article's Creative Commons licence, unless indicated otherwise in a credit line to the material. If material is not included in the article's Creative Commons licence and your intended use is not permitted by statutory regulation or exceeds the permitted use, you will need to obtain permission directly from the copyright holder. To view a copy of this licence, visit <http://creativecommons.org/licenses/by/4.0/>.

References

1. van Ingen Schenau GJ (1982) The influence of air friction in speed skating. *J Biomech* 15(6):449–458. [https://doi.org/10.1016/0021-9290\(82\)90081-1](https://doi.org/10.1016/0021-9290(82)90081-1)
2. Konings MJ, Elferink-Gemser MT, Stoter IK et al (2015) Performance characteristics of long-track speed skaters: a literature review. *Sports Med* 45(4):505–516. <https://doi.org/10.1007/s40279-014-0298-z>
3. Jobse H, Schuurhof R, Cserep F et al (1990) Measurement of push-off force and ice friction during speed skating. *Int J Sport Biomech* 6(1):92–100. <https://doi.org/10.1123/ijsb.6.1.92>
4. Allinger TL, van den Bogert AJ (1997) Skating technique for the straights, based on the optimization of a simulation model. *Med Sci Sports Exerc* 29(2):279–286. <https://doi.org/10.1097/00005768-199702000-00018>
5. van Ingen Schenau GJ, de Boer RW, de Groot G (1987) On the technique of speed skating. *Int J Sport Biomech* 3(4):419–431. <https://doi.org/10.1123/ijsb.3.4.419>
6. de Koning JJ, de Boer RW, de Groot G et al (1987) Push-off force in speed skating. *Int J Sport Biomech* 3(2):103–109. <https://doi.org/10.1123/ijsb.3.2.103>
7. Piuccio T, O'Connell J, Stefanyshyn D et al (2016) Incremental testing design on slide board for speed skaters: comparison between two different protocols. *J Strength Cond Res* 30(11):3116–3121. <https://doi.org/10.1519/JSC.0000000000001392>
8. de Boer RW, Ettema GJC, Faessen BGM et al (1987) Specific characteristics of speed skating: implications for summer training.

- Med Sci Sports Exerc 19(5):504–510. <https://doi.org/10.1249/00005768-198710000-00014>
9. Kandou TWA, Houtman ILD, Bol EVD et al (1987) Comparison of physiology and biomechanics of speed skating with cycling and with skateboard exercise. *Can J Sport Sci* 12(1):31–36
 10. van Ingen Schenau GJ, de Groot G, de Boer RW (1985) The control of speed in elite female speed skaters. *J Biomech* 18(2):91–96. [https://doi.org/10.1016/0021-9290\(85\)90002-8](https://doi.org/10.1016/0021-9290(85)90002-8)
 11. Oriwol D, Milani TL, Maiwald C (2012) Methodological issues associated with the mean value of repeated laboratory running measurements. *Footwear Sci* 4(3):183–190. <https://doi.org/10.1080/19424280.2012.676676>
 12. Allen T, Shepherd J, Wood J et al (2021) Wearables for disabled and extreme sports. In: Stuart S, Godfrey A (eds) *Digital health: exploring use and integration of wearables*. Academic Press, Cambridge, pp 253–273
 13. Houdijk H, de Koning JJ, de Groot G et al (2000) Push-off mechanics in speed skating with conventional skates and klap-skates. *Med Sci Sports Exerc* 32(3):635–641. <https://doi.org/10.1097/00005768-200003000-00013>
 14. Billing DC, Nagarajah CR, Hayes JP et al (2006) Predicting ground reaction forces in running using micro-sensors and neural networks. *Sports Eng* 9(1):15–27. <https://doi.org/10.1007/BF02844259>
 15. Jacobs DA, Ferris DP (2015) Estimation of ground reaction forces and ankle moment with multiple, low-cost sensors. *J Neuroeng Rehabil* 12:90. <https://doi.org/10.1186/s12984-015-0081-x>
 16. Savelberg HHCM, Lange ALHd (1999) Assessment of the horizontal, fore-aft component of the ground reaction force from insole pressure patterns by using artificial neural networks. *Clin Biomech* 14(8):585–592. [https://doi.org/10.1016/S0268-0033\(99\)00036-4](https://doi.org/10.1016/S0268-0033(99)00036-4)
 17. Hill M, Hoena B, Kilian W et al (2016) Wearable, modular and intelligent sensor laboratory. *Proc Eng* 147:671–676. <https://doi.org/10.1016/j.proeng.2016.06.270>
 18. Paredes-Madrid L, Matute A, Pena A (2017) Framework for a calibration-less operation of force sensing resistors at different temperatures. *IEEE Sensors J* 17(13):4133–4142. <https://doi.org/10.1109/JSEN.2017.2706697>
 19. LeCun Y, Bengio Y, Hinton G (2015) Deep learning. *Nature* 521(7553):436–444. <https://doi.org/10.1038/nature14539>
 20. Kamilaris A, Prenafeta-Boldú FX (2018) Deep learning in agriculture: A survey. *Comput Electron Agric* 147(2):70–90. <https://doi.org/10.1016/j.compag.2018.02.016>
 21. Alam M, Samad MD, Vidyaratne L et al (2020) Survey on deep neural networks in speech and vision systems. *Neurocomputing* 417:302–321. <https://doi.org/10.1016/j.neucom.2020.07.053>
 22. Ciulla G, D'Amico A (2019) Building energy performance forecasting: a multiple linear regression approach. *Appl Energy* 253:113500. <https://doi.org/10.1016/j.apenergy.2019.113500>
 23. Wu C, Yu JZ (2018) Evaluation of linear regression techniques for atmospheric applications: the importance of appropriate weighting. *Atmos Meas Tech* 11(2):1233–1250. <https://doi.org/10.5194/amt-11-1233-2018>
 24. Cohen J, Cohen P, West SG et al (2013) *Applied multiple regression/correlation analysis for the behavioral sciences*. Routledge, England
 25. Santiago CB, Guo J-Y, Sigman MS (2018) Predictive and mechanistic multivariate linear regression models for reaction development. *Chem Sci* 9(9):2398–2412. <https://doi.org/10.1039/C7SC04679K>
 26. Chollet F (2018) *Deep learning with Python*. Safari Tech Books Online, Manning, Shelter Island, NY
 27. Nesterov Y (1983) A method for unconstrained convex minimization problem with the rate of convergence $O(1/k^2)$. *Doklady AN USSR* 269:543–547
 28. Sutskever I, Martens J, Dahl G et al (2013) On the importance of initialization and momentum in deep learning. *Int Conf Mach Learn* 28(3):1139–1147
 29. Pedregosa F, Varoquaux G, Gramfort A et al (2011) Scikit-learn: machine learning in Python. *J Mach Learn Res* 12(85):2825–2830
 30. IEE S.A. (2020) Customized input sensing—CIS solutions. DS-CIS-StandardSens-2020-02-11-EN. <https://www.iee-sensing.com/media/download/890/2020-02-11-cis-data-sheet-web.pdf>

Publisher's Note Springer Nature remains neutral with regard to jurisdictional claims in published maps and institutional affiliations.